

# A TEST OF STAR FORMATION LAWS IN DISK GALAXIES

JONATHAN C. TAN<sup>1</sup>

<sup>1</sup>Dept. of Astronomy, University of Florida, Gainesville, Florida 32611, USA

jt@astro.ufl.edu

*Draft version June 21, 2024*

## ABSTRACT

We use observations of the radial profiles of the mass surface density of total,  $\Sigma_g$ , and molecular,  $\Sigma_{\text{H}_2}$ , gas, rotation velocity and star formation rate surface density,  $\Sigma_{\text{sfr}}$ , of the molecular dominated regions of 12 disk galaxies from Leroy et al. to test several star formation laws: a “Kennicutt power law”,  $\Sigma_{\text{sfr}} = A_g \Sigma_{g,2}^{1.5}$ ; a “Constant molecular law”,  $\Sigma_{\text{sfr}} = A_{\text{H}_2} \Sigma_{\text{H}_2,2}$ ; the “Turbulence-regulated laws” of Krumholz & McKee (KM) and Krumholz, McKee & Tumlinson (KMT), a “Kennicutt  $\Omega$  law”,  $\Sigma_{\text{sfr}} = B_\Omega \Sigma_g \Omega$ ; and a shear-driven “GMC collisions law”,  $\Sigma_{\text{sfr}} = B_{\text{CC}} \Sigma_g \Omega (1 - 0.7\beta)$ , where  $\beta \equiv d \ln v_{\text{circ}} / d \ln r$ . We find the constant molecular law, KMT turbulence law and GMC collision law are the most accurate, with an rms error of a factor of 1.5 if the normalization constants are allowed to vary between galaxies. Of these three laws, the GMC collision law does not require a change in physics to account for the full range of star formation activity seen from normal galaxies to circumnuclear starbursts. A single global GMC collision law with  $B_{\text{CC}} = 8.0 \times 10^{-3}$ , i.e. a gas consumption time of 20 orbital times for  $\beta = 0$ , yields an rms error of a factor of 1.8.

*Subject headings:* stars: formation — galaxies: evolution

## 1. INTRODUCTION

Understanding the rate at which stars form from gas is of fundamental importance for a theory of galaxy evolution. At the moment it is uncertain what physical process or processes drive star formation rates (SFRs). Locally, we know star formation occurs mostly in highly clustered,  $\sim$ parsec-scale regions within giant molecular clouds (GMCs) (Lada & Lada 2003; Gutermuth et al. 2009). This clustered mode appears to also be important in a wide range of galactic environments, including dwarf irregular galaxies (Dowell, Buckalew, & Tan 2008), normal disk galaxies (Larsen 2009), and starburst galaxies (Fall et al. 2005; McCrady & Graham 2007). The total efficiency,  $\epsilon$ , of conversion of gas into stars in these clusters is relatively high, with  $\epsilon \sim 0.1 - 0.5$ . However, on the scale of GMCs star formation occurs at a relatively slow, inefficient rate, such that only a few percent of the GMC mass is converted to stars per free-fall time (Zuckerman & Evans 1974; Krumholz & Tan 2007). Although GMCs appear to be gravitationally bound and virialized (Solomon et al. 1987; Bolatto et al. 2008), at any given time, most of the mass and volume of GMCs is not forming stars, perhaps because it is magnetically subcritical (e.g. Heyer et al. 2008).

Starting with the pioneering work of Schmidt (1959, 1963), empirical correlations have been found between the disk plane surface density of SFR,  $\Sigma_{\text{sfr}}$ , and the surface density of gas — either the total,  $\Sigma_g$ , or just that in the molecular phase,  $\Sigma_{\text{H}_2}$ . Based on about 100 disk averages of nearby galaxies and circumnuclear starbursts, Kennicutt (1998, hereafter K1998) found

$$\Sigma_{\text{sfr}} = A_g \Sigma_{g,2}^{\alpha_g}, \quad (1)$$

with  $A_g = 0.158 \pm 0.044 M_\odot \text{ yr}^{-1} \text{ kpc}^{-2}$ ,  $\Sigma_{g,2} = \Sigma_g / 100 M_\odot \text{ pc}^{-2}$ , and  $\alpha_g = 1.4 \pm 0.15$ . Most of the dynamic range determining this relation covers the molecular dominated conditions of the disks in the centers of normal galaxies and in starbursts. Kennicutt et al. (2007) found a similar relation applied on  $\sim$ kpc scales in M51a. Theoretical and numerical models that relate the SFR to the growth rate of large scale gravitational instabilities in a disk predict  $\alpha_g \simeq 1.5$  (e.g. Larson 1988; Elmegreen 1994, 2002; Wang & Silk 1994; Li, Mac Low, & Klessen 2006), as long as the gas scale height does not vary much from galaxy to galaxy. However, the growth rate of large scale instabilities that lead to the formation of GMCs cannot be the rate limiting step for star formation in disks that already have most of their gas mass in the molecular phase in the form of gravitationally bound GMCs. Rather, one should consider the processes that create the actively star-forming, presumably magnetically supercritical, parsec-scale *clumps* of gas within GMCs, which then become star clusters.

Based on a study of 12 nearby disk galaxies at 800 pc resolution, Leroy et al. (2008) (see also Bigiel et al. 2008) concluded that

$$\Sigma_{\text{sfr}} = A_{\text{H}_2} \Sigma_{\text{H}_2,2}, \quad (2)$$

with  $A_{\text{H}_2} = (5.25 \pm 2.5) \times 10^{-2} M_\odot \text{ yr}^{-1} \text{ kpc}^{-2}$  and  $\Sigma_{\text{H}_2,2} = \Sigma_{\text{H}_2} / 100 M_\odot \text{ pc}^{-2}$ . The values of  $\Sigma_{\text{H}_2}$  covered a range from  $\sim 4 - 100 M_\odot \text{ pc}^{-2}$ . They suggest these results indicate that GMCs in these galaxies have approximately uniform properties, e.g. density, and thus are forming stars at a constant rate per free-fall time, as is expected if they are supersonically turbulent (Krumholz & McKee 2005, hereafter KM2005). However, to explain the K1998 data for higher  $\Sigma_g$  systems would require a change in the cloud properties to allow them to form stars at a faster rate.

KM2005 extended their model of turbulence-regulated star formation to predict galactic star formation rates by assuming GMCs are virialized and that their surfaces are in pressure equilibrium with the large scale interstellar medium (ISM) pressure of a Toomre (1964)  $Q \simeq 1.5$  disk, predicting

$$\Sigma_{\text{sfr}} = A_{\text{KM}} f_{\text{GMC}} \phi_{\bar{P},6}^{0.34} Q_{1.5}^{-1.32} \Omega_0^{1.32} \Sigma_{g,2}^{0.68}, \quad (3)$$

with  $A_{\text{KM}} = 9.5 M_{\odot} \text{ yr}^{-1} \text{ kpc}^{-2}$ ,  $f_{\text{GMC}}$  the mass fraction of gas in GMCs,  $\phi_{\bar{P},6}$  the ratio of the mean pressure in a GMC to the surface pressure here normalized to a fiducial value of 6 but estimated to vary as  $\phi_{\bar{P}} = 10 - 8f_{\text{GMC}}$ ,  $Q_{1.5} = Q/1.5$ , and  $\Omega_0$  being  $\Omega$ , the orbital angular frequency, in units of  $\text{Myr}^{-1}$ . We will assume  $f_{\text{GMC}} = \Sigma_{\text{H}_2}/\Sigma_g$  based on resolved studies of GMC populations and molecular gas content in the Milky Way and nearby galaxies (Solomon et al. 1987; Blitz et al. 2007).

Krumholz, McKee & Tumlinson (2009a, hereafter KMT2009) presented a two component star formation law

$$\Sigma_{\text{sfr}} = A_{\text{KMT}} f_{\text{GMC}} \Sigma_{g,2} \times \begin{cases} (\Sigma_g/85 M_{\odot} \text{ pc}^{-2})^{-0.33}, & \Sigma_g < 85 M_{\odot} \text{ pc}^{-2} \\ (\Sigma_g/85 M_{\odot} \text{ pc}^{-2})^{0.33}, & \Sigma_g > 85 M_{\odot} \text{ pc}^{-2} \end{cases} \quad (4)$$

with  $A_{\text{KMT}} = 3.85 \times 10^{-2} M_{\odot} \text{ yr}^{-1} \text{ kpc}^{-2}$ . GMCs are assumed to be in pressure equilibrium with the ISM only in the high  $\Sigma_g$  regime. At low regime, GMCs are assumed to have constant internal pressures set by H II region feedback (Matzner 2002).

K1998 showed that, in addition to being fit by eq. (1), his galaxy and circumnuclear starburst data could be just as well described by

$$\Sigma_{\text{sfr}} = B_{\Omega} \Sigma_g \Omega \quad (5)$$

where  $B_{\Omega} = 0.017$  and  $\Omega$  is evaluated at the outer radius that is used to perform the disk averages. Equation (5) implies that a fixed fraction, about 10%, of the gas is turned into stars every outer orbital timescale of the star-forming disk and motivates theoretical models that relate star formation activity to the dynamics of galactic disks. Such models are appealing as their predicted star formation activity per unit gas mass, i.e. the gas consumption time, is self-similar, depending only on the local orbital time. Examples of these models include those in which star formation is triggered by passage of gas through spiral density waves (e.g. Wyse & Silk 1989). However, there is no evidence that galactic SFRs depend on density wave amplitude (e.g. Kennicutt 1989). Rather, where present, density waves simply help organize gas and star formation within a galaxy.

Noting that in the main star-forming parts of galactic disks a large fraction of total gas is associated with gravitationally bound GMCs and that most stars form in clustered regions in these clouds, Tan (2000, hereafter T2000) proposed a model of star formation triggered by GMC collisions in a shearing disk, which reproduces eq. (5) in the limit of a flat rotation curve since the collision time is found to be a short and approximately constant fraction,  $\sim 20\%$ , of the orbital time,  $t_{\text{orbit}}$ . The collision times of GMCs in the numerical simulations of Tasker & Tan (2009) confirm these results. The T2000 model assumes a Toomre  $Q$  parameter of order unity in the star-forming part of the disk, a significant fraction (e.g.  $\sim 1/2$ ) of total gas in gravitationally bound clouds, and a velocity dispersion of these clouds set by gravitational scattering (Gammie et al. 1991). Then, the predicted SFR is

$$\Sigma_{\text{sfr}} = B_{\text{CC}} Q^{-1} \Sigma_g \Omega (1 - 0.7\beta), \quad (\beta \ll 1) \quad (6)$$

where  $\beta \equiv d \ln v_{\text{circ}} / d \ln r$  and  $v_{\text{circ}}$  is the circular velocity at a particular galactocentric radius  $r$ . Note  $\beta = 0$  for a flat rotation curve. There is a prediction of reduced SFRs compared to eq. (5) in regions with reduced shear, i.e. typically the inner parts of disk galaxies.

Leroy et al. (2008) (see also Wong & Blitz 2002; Bigiel et al. 2008) examined the applicability of the above star formation laws for the galaxies in their sample. In this Letter we revisit this issue, concentrating on the radial profiles of the molecular dominated regions of the 12 disk galaxies studied by Leroy et al.

## 2. METHODOLOGY

We consider the data on  $\Sigma_{\text{sfr}}$ ,  $\Sigma_g$ ,  $\Sigma_{\text{H}_2}$ ,  $\Omega$  and  $\beta$  for the 12 large disk galaxies (see Table 1) analyzed by Leroy et al. (2008), and we refer the reader to this paper for the details of how these quantities were estimated. Note that  $\Omega$  and  $\beta$  depend on the estimated rotation curves of the galaxies. The Leroy et al. (2008) analysis uses analytic fits to the observed rotation curves, since the derivatives of the actual observed curves can be very noisy.

We only consider regions where the molecular gas dominates over atomic, i.e.  $\Sigma_{\text{H}_2} > \Sigma_{\text{HI}}$ , since it is here that we expect a significant fraction of the total gas to be associated with gravitationally bound clouds — an assumption of the T2000 and KM2005 theories — and since we also wish to avoid regions affected by star formation thresholds (Martin & Kennicutt 2001). This requirement defines an outer radius,  $r_{\text{out}}$ , for each galaxy. Note that NGC 2841 has no detected gas in its central region out to about 3.5 kpc, so we only consider annuli from this radius out to  $r_{\text{out}}$  for this galaxy. The requirement that  $\Sigma_{\text{H}_2} > \Sigma_{\text{HI}}$  also leads us to exclude analysis of the 11 H I dominated, low-mass galaxies in the Leroy et al. (2008) sample, which have only upper limits on  $\Sigma_{\text{H}_2}$ .

We use these data to compare the predicted  $\Sigma_{\text{sfr,theory}}$  from: a “Kennicutt power law” with  $\alpha_g = 1.5$  (eq. 1); a “Constant molecular law” (eq. 2); a “KM2005 turbulence-regulated law” (eq. 3); a “KMT2009 turbulence-regulated law” (eq. 4) a “Kennicutt  $\Omega$  law” (eq. 5); and a “GMC collision law” (eq. 6), with the observed values,  $\Sigma_{\text{sfr,obs}}$ , averaged in annuli of typical width  $\sim 500$  pc. For each galaxy and each star formation law we derive the best fit values of  $A_g$ ,

$A_{\text{H2}}$ ,  $A_{\text{turb}}$ ,  $B_{\Omega}$  and  $B_{\text{CC}}$ , respectively, weighting all  $N_{\text{ann}}$  annuli equally, and we measure the rms factor by which the theoretical model errs in estimating the SFR as  $10^{\chi}$ , where  $\chi^2 \equiv (N_{\text{ann}} - N_{\text{fit}})^{-1} \sum (\log R_{\text{sfr}})^2$ ,  $R_{\text{sfr}} = \Sigma_{\text{sfr,theory}} / \Sigma_{\text{sfr,obs}}$  and  $N_{\text{fit}} = 1$ . We also derive values of  $\chi$  for the entire galaxy sample for the case where each galaxy is allowed one free parameter ( $N_{\text{fit}} = 12$ ) and for the case where there is a single star formation law with one free parameter. As discussed by KM2005, these are not traditional  $\chi^2$  goodness-of-fit statistics, but the factor  $10^{\chi}$  does give a measure of how well the theoretical model reproduces the observed system. Note that the models vary in the number of observables they depend on and so measurement errors will introduce varying degrees of dispersion.

### 3. RESULTS & DISCUSSION

Figure 1 shows an example of our method applied to galaxy NGC 3521, displaying the observed profiles of molecular, atomic and total gas content,  $v_{\text{circ}}$ ,  $\beta$ , observed and predicted  $\Sigma_{\text{sfr}}$  and  $R_{\text{sfr}}$ . In this galaxy the star formation laws based on conversion of molecular gas at fixed rate and based on GMC collisions provide the best fit to the observations.

Figure 2 shows  $R_{\text{sfr}}$  for the entire sample of disk galaxies and Table 1 lists the best fit parameters of these models and their dispersions in  $\log R_{\text{sfr}}$ . In order of decreasing accuracy the models are KMT2009 turbulence-regulated, constant molecular, GMC collisions, Kennicutt power law, Kennicutt  $\Omega$  and KM2005 turbulence-regulated, although we caution that given the systematic uncertainties and the different number of observables associated with each law some of these distinctions are probably not significant. Nevertheless, with the freedom to adjust one parameter for each galaxy, which can account for certain systematics such as distance uncertainties, global metallicity variations, foreground extinctions, etc., the KMT2009 turbulence-regulated, constant molecular and GMC collision models can reproduce the observed star formation rates with rms errors of factors of 1.5 (factors of about 1.7 for a single parameter star formation law), while the other models do somewhat worse, e.g. factors of about 2.0 for the KM2005 turbulence-regulated model. We note that the constant molecular law is not a theoretical model that attempts to explain the full Kennicutt relation extending to circumnuclear starbursts. Also this law and the turbulence-regulated laws have had the advantage of using the observed fraction of molecular gas as an input. If the KMT2009 law uses the molecular fractions predicted from the observed metallicities (Krumholz, McKee, & Tumlinson 2009b), the value of  $\chi_{\text{KMT}}$  rises to 0.17 and 0.25 for  $N_{\text{fit}} = 12, 1$ , respectively (with  $A_{\text{KMT}} = 0.038$ ).

In addition to the rms dispersion we note that there are systematic trends with  $r$ : many of the models tend to over predict SFRs in the galactic centers and under predict in outer regions. The centers are where  $\beta$  is relatively large, i.e. of reduced shear, for which the T2000 model for GMC collisions (eq. 6) is not expected to be particularly accurate. Future numerical simulations, extending the analysis of Tasker & Tan (2009), can more accurately measure the dependence of the GMC collision rate as a function of  $\beta$  to help develop a more refined model. Note also that in the limit of pure solid body rotation the GMC collision law needs to be modified to include a mode of star formation not set by shear-driven collisions, i.e. perhaps regulated by magnetic fields or turbulence.

We conclude that a model of star formation controlled by shear-driven GMC collisions,  $\Sigma_{\text{sfr}} = 8.0 \times 10^{-3} Q^{-1} \Sigma_g \Omega (1 - 0.7\beta)$ , is a simple and physically well-motivated model for explaining SFRs in the molecular dominated regions of disk galaxies and circumnuclear starbursts, and is a better description of the radial profiles of  $\Sigma_{\text{sfr}}$  in disk galaxies compared to models based solely on the total gas content and angular velocity, or the KM2005 turbulence-regulated model. For the latter, we note that our best fit value of  $A_{\text{KM}}$  is 1.57, a factor of 6 smaller than predicted by the theory of KM2005, which may indicate other physical effects such as magnetic field support are playing an important role in supporting GMCs and reducing the star formation efficiency (e.g. McKee 1989). Future high angular resolution studies with ALMA to measure kinematics of individual GMCs and to measure galactic radial profiles of velocity dispersion and thus  $Q$  will improve our

TABLE 1  
STAR FORMATION LAW PARAMETERS FOR SAMPLE GALAXIES

| Galaxy<br>NGC:      | d<br>(Mpc) | $r_{\text{out}}$<br>(kpc) | $N_{\text{ann}}$ | $A_g^a$<br>( $10^{-2}$ ) | $\chi_g$<br>( $10^{-2}$ ) | $A_{\text{H2}}^a$<br>( $10^{-2}$ ) | $\chi_{\text{H2}}$<br>( $10^{-2}$ ) | $A_{\text{KM}}^a$ | $\chi_{\text{KM}}$<br>( $10^{-2}$ ) | $A_{\text{KMT}}^a$<br>( $10^{-2}$ ) | $\chi_{\text{KMT}}$<br>( $10^{-2}$ ) | $B_{\Omega}$<br>( $10^{-3}$ ) | $\chi_{\Omega}$<br>( $10^{-2}$ ) | $B_{\text{CC}}$<br>( $10^{-3}$ ) | $\chi_{\text{CC}}$<br>( $10^{-2}$ ) |
|---------------------|------------|---------------------------|------------------|--------------------------|---------------------------|------------------------------------|-------------------------------------|-------------------|-------------------------------------|-------------------------------------|--------------------------------------|-------------------------------|----------------------------------|----------------------------------|-------------------------------------|
| 628                 | 7.3        | 3.7                       | 11               | 11.0                     | 6.71                      | 6.41                               | 11.8                                | 0.750             | 32.1                                | 3.75                                | 10.0                                 | 4.05                          | 22.9                             | 5.37                             | 11.8                                |
| 2841                | 14.1       | 7.9                       | 7                | 14.0                     | 8.72                      | 5.50                               | 7.53                                | 1.07              | 16.2                                | 2.22                                | 5.83                                 | 6.00                          | 8.39                             | 6.01                             | 8.28                                |
| 3184                | 11.1       | 5.1                       | 10               | 7.43                     | 4.40                      | 4.63                               | 9.87                                | 1.60              | 15.5                                | 2.80                                | 12.1                                 | 6.43                          | 9.68                             | 11.7                             | 11.7                                |
| 3198                | 13.8       | 1.7                       | 3                | 27.0                     | 10.1                      | 14.9                               | 8.58                                | 4.82              | 17.6                                | 7.69                                | 18.6                                 | 20.2                          | 19.6                             | 48.3                             | 26.5                                |
| 3351                | 10.1       | 4.7                       | 10               | 23.4                     | 27.1                      | 10.6                               | 14.4                                | 1.57              | 7.14                                | 5.12                                | 24.8                                 | 8.85                          | 8.67                             | 10.9                             | 13.3                                |
| 3521                | 10.7       | 6.5                       | 13               | 5.19                     | 4.56                      | 4.22                               | 1.97                                | 1.25              | 20.6                                | 3.14                                | 5.19                                 | 4.64                          | 13.0                             | 6.26                             | 2.11                                |
| 3627                | 9.3        | 7.4                       | 17               | 8.32                     | 34.2                      | 5.77                               | 25.3                                | 2.08              | 35.4                                | 3.77                                | 24.9                                 | 7.90                          | 36.8                             | 9.90                             | 25.7                                |
| 4736                | 4.7        | 1.7                       | 8                | 14.8                     | 21.8                      | 13.8                               | 20.5                                | 1.02              | 40.9                                | 10.8                                | 10.2                                 | 4.82                          | 33.8                             | 5.34                             | 27.2                                |
| 5055                | 10.1       | 8.6                       | 18               | 4.88                     | 16.3                      | 3.92                               | 10.5                                | 1.51              | 34.9                                | 2.76                                | 8.88                                 | 5.22                          | 29.9                             | 5.82                             | 21.1                                |
| 5194                | 8.0        | 6.0                       | 16               | 5.79                     | 28.7                      | 5.84                               | 25.8                                | 1.71              | 36.7                                | 4.50                                | 20.9                                 | 5.64                          | 33.1                             | 6.76                             | 26.1                                |
| 6946                | 5.9        | 5.9                       | 21               | 6.88                     | 29.1                      | 6.45                               | 19.5                                | 2.59              | 29.0                                | 4.73                                | 17.5                                 | 8.31                          | 29.4                             | 11.5                             | 18.2                                |
| 7331                | 14.7       | 6.8                       | 10               | 7.47                     | 5.61                      | 4.93                               | 2.74                                | 1.26              | 26.7                                | 3.31                                | 5.09                                 | 5.39                          | 17.2                             | 6.98                             | 5.14                                |
| $N_{\text{fit}}=12$ |            |                           | 144              |                          | 22.1                      |                                    | 16.8                                |                   | 29.7                                |                                     | 16.1                                 |                               | 26.3                             |                                  | 18.8                                |
| $N_{\text{fit}}=1$  |            |                           | 144              | 8.17                     | 29.4                      | 5.95                               | 22.2                                | 1.57              | 32.8                                | 3.92                                | 21.8                                 | 6.24                          | 28.4                             | 8.05                             | 24.9                                |

<sup>a</sup>Units:  $M_{\odot} \text{yr}^{-1} \text{kpc}^{-2}$

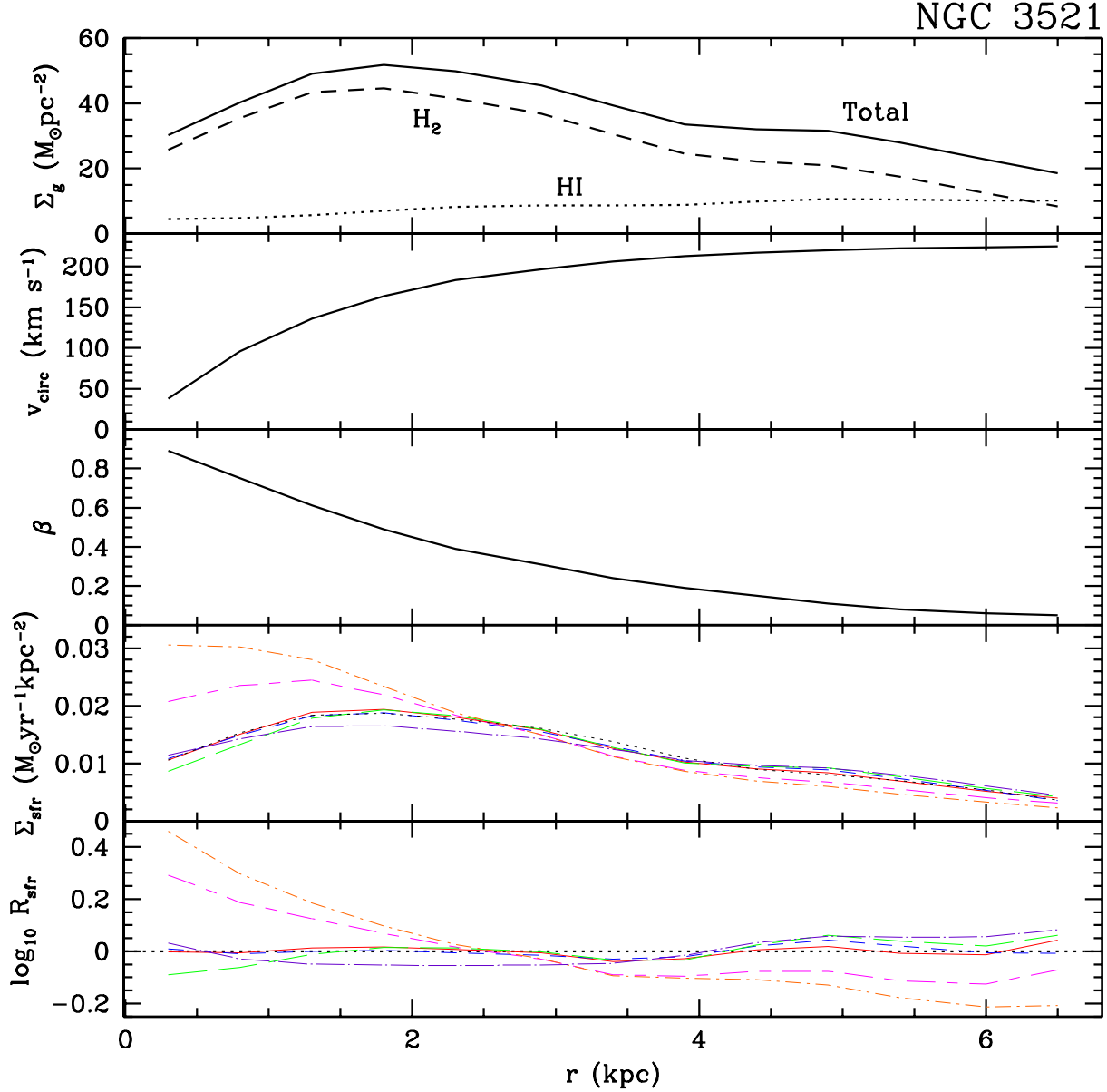


FIG. 1.— Radial distribution of properties of NGC 3521 from Leroy et al. (2008) over the region where molecular gas mass dominates over atomic. First (top) panel: Mass surface densities of total gas,  $\Sigma_g$  (solid), molecular phase including He,  $\Sigma_{H_2}$  (dashed), and atomic phase including He,  $\Sigma_{HI}$  (dotted). Second panel: Circular velocity,  $v_{\text{circ}}$ . Third panel: logarithmic derivative of rotation curve,  $\beta \equiv d \ln v_{\text{circ}} / d \ln r$ . Fourth panel: Star formation rate surface density,  $\Sigma_{\text{sfr}}$ : observed (dotted), predicted via  $\Sigma_{\text{sfr}} = A_g \Sigma_g^{1.5}$  (green long-dashed), via  $\Sigma_{\text{sfr}} = A_{H_2} \Sigma_{H_2,2}$  (blue dashed), via  $\Sigma_{\text{sfr}} = A_{\text{KM}} f_{\text{GMC}} \phi_{P,6}^{0.34} Q_{1.5}^{-1.32} \Omega_0^{1.32} \Sigma_{g,2}^{0.68}$  (orange dot-dashed), via the KMT2009 turbulence law (eq. 4) (purple dot-long-dashed), via  $\Sigma_{\text{sfr}} = B_\Omega \Sigma_g \Omega$  (magenta dashed-long-dashed), and via  $\Sigma_{\text{sfr}} = B_{\text{CC}} \Sigma_g \Omega (1 - 0.7\beta)$  (red solid). Fifth (bottom) panel: Ratio,  $R_{\text{sfr}}$ , of predicted to observed star formation rate surface densities, with line types as in the fourth panel. In this galaxy, the constant molecular (blue dashed) and GMC collision (red solid) star formation laws are the most accurate at predicting the radial profile of  $\Sigma_{\text{sfr}}$ .

ability to test these star formation laws.

We thank Adam Leroy and Mark Krumholz for discussions and Adam Leroy for providing his published data in a convenient format. JCT acknowledges support from NSF CAREER grant AST-0645412.

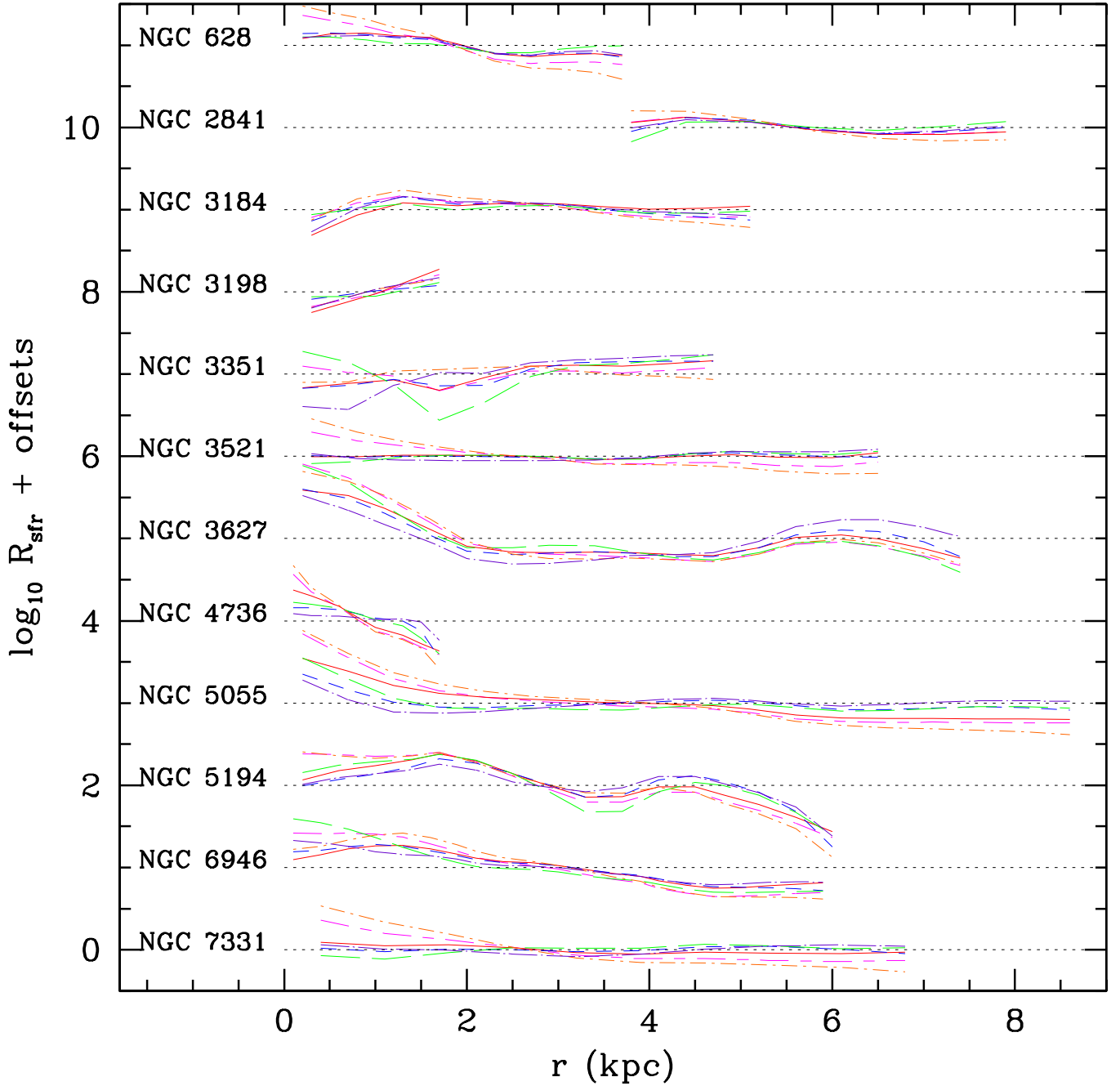


FIG. 2.— Ratio,  $R_{\text{sfr}}$ , of predicted to observed star formation rate surface densities for the entire sample of disk galaxies, offset from each other for clarity: the dotted lines indicate  $R_{\text{sfr}} = 1$  for each galaxy. The line styles are as in Figure 1.

#### REFERENCES

- Bigiel, F., Leroy, A., Walter, F., Brinks, E., De Blok, W. J. G., Madore, B., & Thornley, M. D. 2008, *AJ*, 136, 2846
- Blitz, L., Fukui, Y., Kawamura, A., Leroy, A., Mizuno, N., & Rosolowsky, E. 2007, in *Protostars & Planets V*, eds. B. Reipurth, D. Jewitt, & K. Keil, (U. Arizona: Tucson), p.81
- Bolatto, A., D., Leroy, A. K., Rosolowsky, E., Walter, F., Blitz, L. 2008, *ApJ*, 686, 948
- Dowell, J. D., Buckalew, B. A., & Tan, J. C. 2008, *AJ*, 135, 823
- Elmegreen, B. G. 1994, *ApJ*, 425, L73
- Elmegreen, B. G. 2002, *ApJ*, 577, 206
- Fall, S., Chandar, R., & Whitmore, B. 2005, *ApJ*, 631, L133
- Gammie, C. F., Ostriker, J. P., & Jog, C. J. 1991, *ApJ*, 378, 565
- Gutermuth, R. A., Megeath, S. T., Myers, P. C., Allen, L. E., Pipher, J. L., Fazio, G. G. 2009, *ApJS*, in press, (arXiv:0906.0201)
- Heyer, M., Gong, H., Ostriker, E., & Brunt, C. 2008, *ApJ*, 680, 420
- Kennicutt, R. C., Jr. 1989, *ApJ*, 344, 685
- Kennicutt, R. C., Jr. 1998, *ApJ*, 498, 541 (K1998)

- Kennicutt, R. C., Jr., Calzetti, D., Walter, F., Helou, G., Hollenbach, D. J. et al. 2007, ApJ, 671, 333
- Krumholz, M. R., & McKee, C. F. 2005, ApJ, 630, 250 (KM2005)
- Krumholz, M. R., McKee, C. F., & Tumlinson, J. 2009a, ApJ, 699, 850 (KMT2009)
- Krumholz, M. R., McKee, C. F., & Tumlinson, J. 2009b, ApJ, 693, 216
- Krumholz, M. R., & Tan, J. C. 2007, ApJ, 654, 304
- Larsen, S. S. 2009, A&A, 494, 539
- Larson, R.B. 1988, in *Galactic and Extragalactic Star Formation*, ed. R.E. Pudritz & M. Fich, Dordrecht: Kluwer, 435
- Leroy, A. K., Walter, F., Brinks, E., Bigiel, F., de Blok, W. J. G., Madore, B., & Thornley, M. D. 2008, AJ, 136, 2782
- Li, Y., Mac Low, M.-M., & Klessen, R. S. 2006, ApJ, 639, 879
- Martin, C. L., & Kennicutt, R. C. 2001, ApJ, 555, 301
- Matzner, C. D. 2002, ApJ, 566, 302
- McCady, N., & Graham, J. R. 2007, ApJ, 663, 844
- McKee, C. F. 1989, ApJ, 345, 782
- Schmidt, M. 1959, ApJ, 129, 243
- Schmidt, M. 1963, ApJ, 137, 758
- Solomon, P. M., Rivolo, A. R., Barrett, J., Yahil, A. 1987, ApJ, 319, 730
- Tan, J. C. 2000, ApJ, 536, 173 (T2000)
- Tasker, E. J., & Tan, J. C. 2009, ApJ, accepted
- Toomre, A. 1964, ApJ, 139, 1217
- Wang, B., & Silk, J. 1994, ApJ, 427, 759
- Wong, T., & Blitz, L. 2002, ApJ, 569, 157
- Wyse, R. F. G., & Silk, J. 1989, ApJ, 339, 700
- Zuckerman, B., & Evans, N. J., II. 1974, ApJ, 192, L149